This is a repository copy of *Lithium isotopes in fluid inclusions as tracers of crustal fluids: An exploratory study*.

White Rose Research Online URL for this paper:
http://eprints.whiterose.ac.uk/123384/

Version: Accepted Version

Accepted Manuscript

Lithium isotopes in fluid inclusions as tracers of crustal fluids: An exploratory study

Antonin Richard, David A. Banks, Nina Hendriksson, Yann Lahaye

Please cite this article as: Antonin Richard, David A. Banks, Nina Hendriksson, Yann Lahaye , Lithium isotopes in fluid inclusions as tracers of crustal fluids: An exploratory study. The address for the corresponding author was captured as affiliation for all authors. Please check if appropriate. Gexplo(2017), doi:10.1016/j.gexplo.2017.10.017

Lithium isotopes in fluid inclusions as tracers of crustal fluids: An exploratory study

Antonin Richard [a,b*], David A. Banks [c], Nina Hendriksson [a], Yann Lahaye [a]

[a] Geological Survey of Finland (GTK), P.O. Box 96, FI-02151 Espoo, Finland

[b] Université de Lorraine, CNRS, CREGU, GeoRessources, Vandoeuvre-lès-Nancy, F-54506, France

[c] School of Earth and Environment, University of Leeds, Woodhouse Lane, Leeds, LS2 9JT, UK

* Corresponding author: Antonin Richard, GeoRessources UMR 7359, Université de Lorraine, Faculté des Sciences et Technologies, Entrée 3B - bureau A609, Boulevard des Aiguillettes BP 70239, 54506 Vandœuvre-lès-Nancy Cedex, France

Phone : +33 3 83 68 47 37

Fax : +33 3 83 68 47 01

Mail : antonin.richard@univ-lorraine.fr

Abstract

Lithium isotopes are extensively used to trace fluid migration and fluid-rock interactions in the shallow Earth's crust. Although, Li isotope systematics might give important information about deep crustal fluids, this stable isotope system remains surprisingly under exploited in fluid inclusions. Here, twenty-three samples from a variety of deep environments, from diagenetic, metamorphic to magmatic-hydrothermal conditions (~ 150 to 600°C), have been investigated in order to provide the first exploratory overview of the range in Li isotopic composition of fluid inclusions. From 1-2 g of hydrothermal quartz or dolomite, cation analysis (Na, K, Ca, Mg, Sr, Li), Li fraction recovery and Li isotopic analysis of bulk fluid inclusion leachates were carried out by using an innovative approach coupling crush-leach extraction, high performance ion chromatography and MC-ICPMS analysis. Reconstructed Li concentrations and δ^7Li values of these fluid inclusions (respectively 12 to 653 mg/l and -1.4 ± 0.2‰ to $+41.3 \pm 0.8$‰) are compatible with previously proposed models for the origin of the fluids and fluid-rock interactions. δ^7Li values are independent from other tracers (Br/Cl, I/Cl) and parameters such as temperature, salinity, and cation content (Na/Ca, Na/K, Na/Mg, Na/Li, Na/Sr ratios). The results show that, in conjunction with other parameters, the Li isotopic compositions of fluid inclusions are potentially powerful source and process tracers of deep crustal fluids within a wide range of geological environments and related ore-forming systems, for example in from sedimentary basins, seafloor hydrothermal systems and subduction zones.

2

1. Introduction

Understanding mass transfer within the Earth's crust requires tracing the origin of deep fluids and their fluid-rock interactions (Yardley and Bodnar, 2014). Ancient deep crustal fluids are preserved in fluid inclusions. However due to the small volume of fluid that is trapped as the host mineral grows, the use of isotopic tracers is challenging (Pettke et al., 1995, 2010; Gleeson et al., 1999; Banks et al., 2000a). With notable exceptions of a few pioneering studies, the Li isotopic composition of fluid inclusions remains largely under-exploited (Teng et al., 2006a; Masukawa et al., 2013; Yang et al., 2015).

Lithium is a moderately incompatible fluid mobile element, with a ionic radius of 0.76 Å (for Li^+) and a large relative mass difference of ~ 16% between the two stable isotopes ^6Li and ^7Li (relative abundances ~ 7.5% and ~ 92.5% respectively). δ^7Li values and Li concentrations of present-day shallow fluids (10^{-4} to 10^2 mg/l in ground waters, geothermal waters, hydrothermal vents) are dominantly controlled by: (i) the initial concentration and isotopic composition of the pristine fluids (e.g. meteoric water, seawater, magmatic water); (ii) release from / incorporation into soil-, sediment- and rock-forming minerals and (iii) fluid-assisted grain-boundary diffusion, as ^6Li diffuses faster than ^7Li (Teng et al., 2006b; Millot et al., 2007a; Scholz et al., 2010; Penniston-Dorland et al., 2010; Schmitt et al., 2012). This results in a wide range of the reported compositions for rocks ($\delta^7Li = -20‰$ to $+25‰$) and fluids ($\delta^7Li = -5‰$ to $+45‰$) (Tomascak et al., 2016). In addition, there is very little fractionation in hydrothermal systems during boiling ($\Delta^7Li_{vapour-liquid} \leq -0.5‰$) and therefore Li isotopes are indicative of the source reservoirs and fluid-rock interactions (Liebscher et al., 2007). Consequently, Li isotopes have huge potential for tracing crustal fluids and have been extensively studied: (i) in submarine hydrothermal vents, geothermal waters and ground waters (Chan et al., 1993; Bottomley et al., 1999; Millot et al.,

3

2007b; (ii) in minerals and whole-rock samples (Chan et al., 1993; Romer et al., 2005; Halama et al., 2011) and (iii) to determine fluid/mineral isotopic fractionation factors (Lynton et al., 2005; Wunder et al., 2007; Jahn and Wunder 2009).

In order to better assess the potential of Li isotopes in fluid inclusions as a tracer of different crustal fluids, twenty-three samples from eight localities worldwide covering diagenetic, metamorphic and magmatic-hydrothermal conditions were selected (Table 1). Samples were first analysed by laser ablation - inductively coupled plasma mass spectrometry (LA-ICPMS) for determination of Li concentration in the minerals (quartz and dolomite) hosting the fluid inclusions. Then, for each sample, a bulk fluid inclusion leachate was extracted using the conventional "crush-leach" method (Banks et al., 2000b). The fluid inclusion leachate was analysed for its cation (Li, Na, Ca, K, Mg, Sr) composition, followed by the separation of Li using automated high-performance ion chromatography (HPIC). The Li elution (and other major cations mention above) was monitored for every samples using HPIC, which guarantees a high elution yield and pure Li separation. Finally, the Li isotopic composition of the eluted Li was analysed by multi collector - inductively coupled plasma mass spectrometry (MC-ICPMS). To the authors' knowledge, this is the first time that a combination of automated HPIC for cation elution and isotopic analysis is used on fluid inclusion leachates.

2. Materials and methods

2.1. Sampling

The samples were selected according to the following criteria: (i) previously-published fluid inclusion data (trapping temperature, composition and origin of the enclosed fluids) is

4

available for all samples, or paragenetically equivalent samples, of one locality (Table 1); (ii)

primary and pseudosecondary fluid inclusions were the dominant and most saline fluid inclusion

population, and therefore comprise by far the majority of the element budget of Li in order that

the data represented a single fluid and not a mixture of fluids; (iii) the samples were selected from

relatively high-permeability hydrothermal vein systems where fluid flow rates were more than

high enough to favor advective over diffusive Li transport (Dolejš et al., 2015); this means that

diffusion between the wall rocks and the fluids prior to fluid inclusion trapping is expected to

have had an insignificant effect on Li concentrations and δ^7Li values and (iv) the dominant fluid

inclusion populations in the samples account for the diversity of temperature and salinity of deep

crustal fluids. Among the selected samples, primary and pseudosecondary fluid inclusions have

reconstructed salinities based on microthermometry of ∼ 5 to 78 wt.% equiv. NaCl and trapping

temperature of ∼ 150 to 600°C.

Twenty-two samples from hydrothermal veins consist of quartz and one consists of

dolomite (sample RBL5Carb). The following sample descriptions were ordered according to their

estimated trapping temperature (low to high). The selected samples include (Table 1): (i) quartz

and dolomite from veins related to circulation of basinal brines from evaporated seawater at the

basement-cover interface around "unconformity-related" U deposits in the Athabasca basin

(Canada) and Kombolgie sandstones (Australia) (Derome et al., 2007; Richard et al., 2011); (ii)

quartz from Cu, Pb, Zn-sulfides-bearing veins spatially associated with cooling Variscan granites

and formed by circulation of, probably, magmatic fluids variably diluted by connate fluids from

the country rocks in Southwest England (Alderton and Harmon, 1991; Turner and Bannon,

1992); (iii) quartz from Au-bearing veins related to metamorphic fluids in the Brusson Au district

(Italy) (Yardley et al., 1993); (iv) quartz from veins related to the infiltration of basinal fluids into

igneous and metamorphic basement rocks of the Modum Complex (Norway) (Munz et al., 1995);

(v) quartz from veins formed by circulation of dominantly meteoric-derived fluids related to the late-stage cooling of a Variscan granite in the Panasqueira W-Sn deposit (Portugal) (Polya et al., 2000); (vi) quartz from veins formed by syntectonic circulation of fluids derived from evaporated seawater along a Pyrenean thrust (central Pyrenees, France) (McCaig et al., 2000); (vii) quartz from Sn, W-oxides-bearing veins associated with Variscan granites and most likely formed from magmatic fluids in Southwest England (Alderton and Harmon, 1991; Turner and Bannon, 1992) and (viii) quartz from Th, U, REE-minerals-bearing veins formed from magmatic fluids introduced in brecciated zones above the Capitan Mountains pluton (New Mexico, U.S.A.) (Campbell et al., 1995).

2.2. Laser ablation - inductively coupled plasma mass spectrometry (LA-ICPMS)

LA-ICPMS analysis of mineral separates mounted on polished sections was carried out at the School of Earth and Environment, University of Leeds (Allan et al., 2005; Allan and Yardley, 2007). Areas devoid of visible fluid inclusions under optical microscope were ablated with a 193 nm Geolas Q Plus excimer laser (ArF, 193 nm, Microlas, Göttingen, Germany). Ablated samples were subsequently analysed in an Agilent 7500c Quadrupole ICP-MS equipped with an Octopole Reaction System. The recorded isotopes were ^{7}Li, ^{27}Al, ^{29}Si and ^{44}Ca, with ^{29}Si used as the internal reference element. For the analysed elements the accuracy is within 15%. NIST silicate glass standard SRM 610 was used as an external calibration standard and NIST SRM 612 used as a check of the analysed Li concentrations. The standard value is 41.54 ± 2.9 µg/g (1σ) and the analysed value was 44.8 ± 2.5 µg/g (1σ). Signal integration was performed with the Matlab®-based SILLS program (Guillong et al., 2008).

2.3. Crush-leach

Samples were crushed in an agate pestle and mortar and leached at the School of Earth and Environment, University of Leeds, UK, to release their bulk fluid inclusion content according to the conventional "crush-leach" technique (Banks et al., 2000b). Samples were crushed to a grain size fraction of 1-2 mm. Pure mineral separates were then picked under a binocular microscope and placed in a ultrasonic bath for 1 hour. Then samples were cleaned by boiling three times in 18.2MΩ de-ionised water. Cleaned quartz and dolomite grains (0.5 to 1.5 g) were crushed to a fine powder in an agate pestle and mortar and the mineral powders were leached in 5-6 ml distilled 18.2 MΩ de-ionised water and filtered immediately, to minimise leaching of Li from the host minerals, using a 0.2 µm nylon filter.

2.4. Ion chromatography (IC)

Samples from Southwest England and Panasqueira Sn-W deposit were analysed for Cl, Br and I at the School of Earth and Environment, University of Leeds, UK, with a Dionex DX-500 ion chromatograph (IC). Anion analyses were not carried out on the other samples for this study because similar analyses on paragenetically equivalent samples have been previously published, as mentioned in Table 1.The detection limit in fluid inclusion leachates is ~ 3 µg/l for Cl and ~ 1 µg/l for Br and I. Molar Br/Cl ratios are quoted with an error of less than ± 5% based on the replicate analysis of a standard seawater sample (Ocean Scientific GPS-1, Atlantic seawater) and I/Cl ratios are semi-quantitative due to the very low concentration of iodine the leachates.

2.5. High-performance ion chromatography (HPIC)

For all samples, leachates from fluid inclusions were analysed for the concentrations of Li, Na, Mg, K, Ca and Sr at the Geological Survey of Finland (GTK, Espoo). Automated separation of Li from the leachates of fluid inclusions were performed using an HPIC technique similar to that previously described for the separation of Sr as applied to natural waters and carbonate rock digests (Meynadier et al., 2006). HPIC separation for Li was performed with the setup consisting of: (i) the temperature and pressure controlled Dionex ICS-3000 ion chromatograph with the Dionex AS autosampler; (ii) the Gilson FC204 fraction collector and (iii) the Chromeleon® monitoring software. The autosampler with a 5 ml injection syringe consists of places with 10 ml sample vials and caps with Teflon covers. Samples were injected through a 500 µl sample loop. A Dionex GC16 guard and CS16 analytical columns in series with the methane sulfonic acid (MSA) eluent were used for the ion-exchange. A high sensitivity for the cation detection was attained by using the self-regenerating Dionex CSRS 300 suppressor. Ion fractions were collected in a fraction collector containing 4×60 seat racks with 8 ml plastic sample tubes. In every step of analysis MQ water of 18.2 MΩ.cm was used (Milli-Q Integral / Q-pod Element Unit). To reach the required degree of Li separation the following parameters were used: 40 mM MSA eluent concentration, column at 50°C, suppressor at 20°C and flow rate of 1 ml/min. The instrument was calibrated for each cation over the following concentration ranges; 0.002 to 0.1 mg/l for Li, 0.2 to 10 mg/l for Na, K and Mg, 0.6 to 30 mg/l for Ca and 0.02 to 1 mg/l for Sr. The calculated limits of detection for Li, Na, Mg, K, Ca and Sr, are respectively 1.12, 110, 15, 212, 3065 and 21 ng/l. Cations concentrations of the fluid inclusion leachates were optimised to the given calibration range. Therefore, dilution or enrichment of the samples was not necessary prior to analysis. Each sample was run between one and five times in order to collect enough Li for the

isotopic analysis. At each sample change, washing of the whole separation line was performed

using MQ water (25 + 10 minutes runs) in order to obtain clean blank runs. The reported

concentrations represent an average of the multiple IC measurements. Cation concentrations in

the fluid inclusion leachates are quoted generally with a 1σ error of less than ± 3% for Li, ± 1%

for Na, ± 3% for Mg, ± 1% for K, ± 2% for Ca and ± 3% for Sr. Absolute Li concentrations in the

bulk fluid inclusion populations are reconstructed from the average salinity estimated from

microthermometry (in wt.% NaCl equiv.; Table 1) using a charge-balance approach, which will

result in a maximum error in the concentrations of only ± 10%. This method corrects the

modelled amount of Na (from the wt.% NaCl equiv.) for contributions from other chloride salts

using the analysed elemental ratios to Na (Allan et al., 2005).

2.6. Multi collector - inductively coupled plasma mass spectrometry (MC-ICPMS)

Lithium isotopic measurements on Li fractions recovered from fluid inclusion leachates

by HPIC were performed at the Geological Survey of Finland (GTK, Espoo). The samples were

evaporated almost to dry and recovered into disposable 2ml beakers in 1.0 to 1.5 ml HNO_3 2%.

The analysis were carried out by using a desolvator nebuliser, a 50μl PFA MicroFlow^{TM}

nebuliser and a MC-ICPMS (Nu Instruments^{TM}) at low mass resolution ($\Delta m/m = 400$). The Li

isotopic measurements were performed in static mode using the two outermost faraday detectors,

and 6 blocks of 10 integrations. The samples were analysed two to three times, depending on the

amount of Li collected by HPIC, and the results are given as an average of the measurements.

Values of $\delta^7 Li$ are reported in standard per mil (‰) notation relative to L-SVEC (a Li pure

carbonate standard NIST RM 8545; Flesch et al., 1973) where $\delta^7 Li = [(^7Li/^6Li)_{sample}/(^7Li/^6Li)_{L-SVEC} - 1] \times 1000$. A laboratory in house Li standard having L-SVEC-like (i.e. 0‰) isotopic

9

composition was run through the HPIC separation setup and generated an average isotopic

composition of -0.04 ± 0.04‰ (n = 3), which indicates negligible (<0.08‰) instrumental

fractionation during combined HPIC and MC-ICPMS.

3. Results

Analytical results are reported in Table 2 and plotted in Fig. 1 and 2 and are briefly

described below.

3.1. Lithium concentration in the host minerals

The Li concentrations in the minerals hosting the fluid inclusions ranges from 0.5 ± 0.1

µg/g (1σ) to 108.8 ± 6.9 µg/g (1σ) in the quartz samples and is of 0.07 ± 0.01 µg/g (1σ) in the

dolomite sample. Within individual samples, the relative standard deviation (RSD) of Li

concentrations is between 4 and 72%. Variation of Li concentration between quartz samples from

the same locality is generally less than a factor of ten. Samples with less than 30 µg/g Li in the

quartz have a maximum of 300 mg/l Li in the enclosed fluid inclusions. As a general observation

samples with more than 40 µg/g Li in the quartz, always have Li concentrations in the enclosed

fluid inclusions between 200 and 650 mg/l (Fig. 2a). The Li concentrations in the mineral host do

not correlate with trapping temperature or δ^7Li values of associated fluid inclusions (Fig. 2b).

3.2. Cation composition of the fluid inclusions

The cation concentrations in the fluid inclusion leachates show the following ranges: Li = 7.5 to 145.7 µg/l, Na = 0.93 to 41.60 mg/l, K = 0.05 to 13.32 mg/l, Mg = 0.01 to 1.26 mg/l, Ca = 0.11 to 20.19 mg/l and Sr = 8.7 to 1135 µg/l. Li concentration in the fluid inclusions reconstructed from the average salinity estimated from microthermometry (see Section 2.5.) range from 12 to 653 mg/l. This is in good agreement with previously published data on equivalent samples (see references in Table 1). Sodium is the dominant cation in the fluid inclusion leachates and Na/cation molar ratios have the following ranges: Na/Li = 13 to 1138, Na/K = 4 to 53, Na/Mg = 2 to 800, Na/Ca = 1 to 23 and Na/Sr = 30 to 5383. Again, this compares well with previously published data on equivalent samples (see references in Table 1). Variation of the Na/cation ratio within individual localities is generally less than a factor of ten.

3.3. Lithium isotopic compositions of the fluid inclusions

The Li isotopic compositions of the fluid inclusion leachates range from -1.4 ± 0.2‰ (1σ) to $+41.3 \pm 0.8$‰ (1σ). The different samples from a given locality typically have a narrow range $(< 8$‰$)$ in δ^7Li values (Southwest England, Brusson, Panasqueira, Central Pyrenees and Athabasca basin). For example, δ^7Li is between $+1.3 \pm 0.5$‰ (1σ) and $+4.7 \pm 0.3$‰ (1σ) in the four samples from the Brusson Au district and between $+8.7 \pm 0.3$‰ (1σ) and $+13.8 \pm 0.2$‰ (1σ) in the four samples from central Pyrenees. However, an exception is the Modum Complex, where δ^7Li values range from $+11.1 \pm 0.3$‰ (1σ) to $+34.7 \pm 0.2$‰ (1σ) in the four analysed samples. The ranges of δ^7Li values may partly or fully overlap between the sample sets of different localities (e.g. Southwest England / Brusson or Athabasca basin / Modum Complex respectively).

11

The majority of compositions do not overlap between the sample sets of different localities in a $\delta^7\text{Li}$ vs [Li] field (Fig. 1). The $\delta^7\text{Li}$ values of fluid inclusions show no clear correlation with trapping temperature and salinity, or Br/Cl, I/Cl, Na/Ca, Na/K, Na/Mg, Na/Li and Na/Sr molar ratios, considering individual localities and for the overall dataset (Fig. 2c-k).

4. Discussion

4.1. Significance of $\delta^7\text{Li}$ values

Here, fluid inclusions are generally significantly enriched in Li compared to their host mineral (Fig. 2a). The fact that the highest Li concentrations in fluid inclusions are associated with the highest Li concentrations in the host quartz may suggest that, for the studied samples, the Li concentration in the hydrothermal fluids controls the Li concentration of the quartz growing in the fluids (Fig. 2a). The range of Li concentrations in quartz of this study is consistent with those previously established in quartz when entirely free of any solid inclusions (Monecke et al., 2002; Götze et al., 2004; Allan and Yardley, 2007). Therefore the Li concentrations in quartz most likely reflect structurally-hosted Li in the quartz lattice.

The solubility of quartz in pure water at 25°C is very low (~ 10 ppm; Tester et al., 1994) and leachates are filtered to remove quartz particles immediately. Assuming an extreme scenario using samples with the lowest $\text{Li}_{\text{leachate}}/\text{Li}_{\text{quartz}}$ ratios (MTE, SW18, LD888, CA 00-1 and RBL5Qz; Table 2), and with 5 ml of leachates for 1 g of crushed quartz, more than 5% contamination of the fluid inclusion leachates by the host quartz may only be observed if more than 0.01% of the total Li of the host quartz is transferred to the leachates during the crush-leach procedure. Therefore such significant contamination is very unlikely.

12

Li may be depleted in the host minerals around fluid inclusions due to dissolution-precipitation reactions associated with Li transfer from quartz to fluid inclusions, as shown in samples similar to those from the Brusson Au district studied here (Lambrecht and Diamond, 2014). Diffusion of Li between fluid inclusions and the host quartz may also occur. However, experiments showing significant diffusion between fluid inclusions and the host quartz have only been carried out at temperatures above 500°C and using concentration gradients much higher that reported here (Zajacz et al., 2009). Within one locality, there is no systematic relationship between Li concentrations in the fluid inclusions and their δ^7Li values (Fig. 1). In addition, δ^7Li values from fluid inclusions trapped inside quartz and dolomite from the Rabbit Lake U deposit (Athabasca basin) are identical within error, while the Li content of quartz and dolomite differ significantly (Table 2). Importantly, the Δ^7Li$_{quartz-fluid}$ values of fluid inclusions and their host quartz from a giant volcanogenic massive sulfide deposit show a strong temperature-dependent isotopic fractionation (between 175°C and 340°C) indicating that fluid inclusions are in isotopic equilibrium with their host quartz (Yang et al., 2015). Collectively this implies that, for the studied samples, neither the Li concentration not isotopic composition are significantly altered by post-entrapment reequilibration with the host mineral.

4.2. Consequences for fluid tracing

4.2.1. Controls on Li concentrations and δ^7Li values

In Figure 1, δ^7Li value and Li concentration of the studied fluid inclusions can be compared with compositions of various fluids (geothermal waters, sediment-hosted diagenetic and hydrothermal fluids, mid-ocean ridge vent fluids), as well as modern seawater, evaporated

13

seawater, meteoric waters and the upper continental crust. Trends between meteoric water,

seawater, evaporated seawater and upper continental crust (UCC) represent binary mixing lines

between the different reservoirs (Scholz et al., 2010). During fluid-rock interaction, clay mineral

formation may alternatively lead to Li release to the fluid phase (Burisch et al., 2016a) or Li

uptake from the fluid phase into the clay minerals (Scholz et al., 2010). Here, Figure 1 shows the

evolution of fluid composition during progressive Li incorporation into authigenic clay minerals

at 150°C and 350°C, calculated using a Rayleigh fractionation model and represented for

different fractions of the initial Li remaining in the fluid (between 1 and 0.1; Scholz et al., 2010).

While most present-day geothermal waters and hydrothermal / vent fluids do not exceed

Li concentrations of ~ 100 mg/l, the fluid inclusions reported here have significantly higher Li

concentration of up to 653 mg/l (Fig. 1). Possible reasons for the distinct Li enrichment in the

fluid inclusions are that the fluid inclusions reported here are either related: (i) to hydrothermal

activity within relatively Li-rich felsic magmatic and metamorphic rocks (Capitan Mountains,

Brusson Au district, Southwest England, Panasqueira, references in Table 1), or (ii) to evaporitic

systems where Li can be concentrated to ~ 40 times the original seawater value in the residual

brine after evaporation beyond halite saturation (Kombolgie sandstones, Athabasca basin, central

Pyrenees and possibly Modum Complex, references in Table 1, seawater evaporation trend in

Fig. 1). Therefore, high Li content of the studied fluid inclusions may originate from: (i) the high

Li content in the pristine fluids and/or the country rocks and (ii) Li leaching (Burisch et al.,

2016a) dominating over Li incorporation (Scholz et al., 2010) into country rocks. More generally,

Li concentration higher than 100 mg/l seem to be the rule rather than the exception in geothermal,

metamorphic and magmatic fluids, even in environments that are not distinctly Li-rich (Yardley,

2005).

In Figure 2, δ^7Li values of the studied fluid inclusions have been plotted against various parameters (trapping temperature, salinity and Br/Cl, I/Cl, Na/Ca, Na/K, Na/Mg, Na/Li and Na/Sr molar ratios). δ^7Li values of fluid inclusions are clearly independent of trapping temperature, even for a given area, in contrast to the strong temperature dependence of δ^7Li values, between ~ 50 and 250°C, observed in some hydro-geothermal systems (Millot et al., 2007a) (Fig. 2c). Although some of the data would be close to the regression line of Millot et al. (2007) if it was extrapolated to the 250-300°C temperature range, this indicates that Li isotope geothermometry may not be applicable to the range of fluid inclusions studied here. The independence of δ^7Li values and Br/Cl and I/Cl values (Fig. 2e,f) confirms that δ^7Li values of fluid inclusions cannot be used as the sole indicator of the fluids origin, and could be used in conjunction with halogen ratios which usually retain information on the source of the fluids but may also be variably affected by water-rock interaction (Kendrick and Burnard, 2013; Burisch et al., 2016b). The independence of δ^7Li values and Na/cation ratios suggests that Li isotopic compositions of the investigated fluids are not dominantly controlled by a single reaction. Rather, Li isotopic compositions of the investigated fluids are most probably controlled by the multiple reactions related to diagenetic, hydrothermal and metamorphic processes involving Li-bearing silicate minerals (e.g. micas, clays) as reactants or products. Therefore, δ^7Li values and Li concentrations of fluid inclusions may preserve information on both the origin of pristine fluids and the degree of interaction with crustal rocks. Further quantitative assessment of the Li budget and isotopic fractionation during fluid-rock interaction in hydrothermal systems could help refine the interpretation of Li concentrations and δ^7Li values of fluid inclusions (Foustoukos et al., 2004; Scholz et al., 2010; Gao et al., 2012) but is beyond the scope of this study.

4.2.2. Magmatic fluids

Fluid inclusions formed from presumably magmatic fluids (Capitan Mountains and Southwest England) have low δ^7Li values, comparable with those of the upper continental crust (UCC, Fig. 1). This is compatible with similar observations from the Takatori W deposit (Japan) and from the Gacun Zn-Pb-Cu deposit (China) (Masukawa et al., 2013; Yang et al., 2015). Fluid inclusions in quartz from the Tin Mountains pegmatite in the Black Hills (U.S.A.) have higher δ^7Li values than those in other fluid inclusions mentioned above (+8.1 to 13.4‰). This has been explained by isotopic fractionation during crystal-melt fractionation during the latest stage of granite differentiation and fluid exsolution (Teng et al., 2006a). Therefore, low δ^7Li values in fluid inclusions from Capitan Mountains and Southwest England are in accordance with the previously proposed genetic models which assume a dominantly magmatic origin of the fluids and Li (Alderton and Harmon, 1991; Turner and Bannon, 1992; Campbell et al., 1995).

4.2.3. Sedimentary fluids

Fluid inclusions formed from fluids related to sedimentary aquifers have high δ^7Li values (Central Pyrenees, Modum Complex, Kombolgie sandstones, Athabasca basin) (Fig. 1). Figure 1 indicates that variations of Li concentrations and δ^7Li values away from the composition of seawater / evaporated seawater towards isotopically lighter and Li-rich compositions may reflect combinations of Li leaching from country rocks and Li incorporation into authigenic clay minerals. This is compatible with previously proposed models for the origin of the fluids which assume seawater / evaporated seawater as fluid sources and with the well-developed alteration haloes around the veins hosting the studied samples (Munz et al., 1995; McCaig et al., 2000;

Derome et al., 2007; Richard et al., 2011). A detailed mass-balance calculation on those haloes would be needed to confirm this hypothesis. In addition, no simple mechanism can explain isotopic compositions heavier than seawater combined with the elevated Li concentrations observed for two of the four samples from the Modum Complex (IA-463, IA-527).

4.2.3. Metamorphic and meteoric-derived fluids

Fluid inclusions formed from fluids originating from meteoric water dominantly (Panasqueira) and metamorphic fluids (Brusson) have δ^7Li values intermediate between fluid inclusions formed from magmatic fluids and fluid inclusions formed from sedimentary fluids (Fig. 1). Although the ultimate origin of fluids from Brusson has been disputed, the δ^7Li values indicate that most of the Li results from leaching in some metamorphic wall rocks, as suggested by the alteration haloes along the veins hosting the studied quartz (Yardley et al., 1993; Pettke et al., 2000), similarly to what is observed in other vein systems hosted in crystalline rocks (Burisch et al., 2016a). At Panasqueira, Figure 1 indicates that δ^7Li values values may be influenced either by (i) meteoric water and additional leaching of crustal Li or (ii) magmatic fluid as a source. However, based on noble gas and halogen analyses, a magmatic source would be very minor (Polya et al., 2000) compared to meteoric water. Moreover an additional process is required to account for δ^7Li values above the upper crust composition. It can be speculated that this additional process could be Li incorporation into micas in the vein systems hosting the studied quartz (sample MSS/PAS 2) as suggested by the intense alteration developed around the W-Sn deposit (Polya et al., 2000). Due to their initially low Li concentration, fluids originating from meteoric water dominantly (Panasqueira) and metamorphic fluids (Brusson) are expected to be strongly influenced by leaching of upper crustal Li and fluid mixing. Here, this is verified by

17

their relatively light Li isotopic compositions close to magmatic fluids and the upper continental crust.

5. Perspectives

For the studied samples, Li concentration and δ^7Li values of fluid inclusions are compatible with previously proposed genetic models for the origin of the fluids and fluid-rock interactions. δ^7Li values are independent from other tracers (e.g. Br/Cl, I/Cl) and other parameters (e.g. temperature, salinity, Na/Ca, Na/K, Na/Mg, Na/Li and Na/Sr). Therefore, Li isotopes in fluid inclusions provide valuable information that can be used in combination with other geochemical tracers to better constrain the origin of fluids and the mode of fluid-rock interaction.

Potential areas where the determination of Li isotopes could be used as tracers of crustal fluids include: (i) subduction zones, where Li is an indicator of slab dehydration and metasomatic processes (Chan and & Kastner, 2000; Penniston-Dorland et al., 2012); (ii) seafloor hydrothermal systems where Li is an indicator of seawater / oceanic crust interaction (Foustoukos et al., 2004; Gao et al., 2012) and (iii) ore-forming magmatic-hydrothermal systems where Li is an indicator of magmatic and metasomatic processes but also a metal of economic interest (Deveaud et al., 2015). Finally, the analysis of fluid inclusions provides direct access to the Li isotopic composition of deep crustal fluids that are not obtainable by direct sampling, and can provide valuable information that may help understanding Li transfer between the hydrosphere, the crust and the mantle, via fluids and magmas.

18

Acknowledgements

References

Alderton, D. H. M. & Harmon, R. S. Fluid inclusion and stable isotope evidence for the origin of mineralizing fluids in south-west England. Mineral. Mag. 55, 605–611 (1991).

Allan, M. M., Yardley, B. W. D., Forbes, L. J., Shmulovich, K. I., Banks, D. A. & Shepherd, T.J. Validation of LA-ICP-MS fluid inclusion analysis with synthetic fluid inclusions. Am. Mineral. 90, 1767–1775 (2005).

Allan, M. M. & Yardley, B. W. D. Tracking meteoric infiltration into a magmatic-hydrothermal system: A cathodoluminescence, oxygen isotope and trace element study of quartz from Mt. Leyshon, Australia. Chem. Geol. 240, 343–360 (2007).

Banks, D. A., Green, R., Cliff, R. A. & Yardley, B. W. D. Chlorine isotopes in fluid inclusions: determination of the origins of salinity in magmatic fluids. Geochim. Cosmochim. Acta 64, 1785–1789 (2000a).

Banks, D. A. Giuliani, G., Yardley, B. W. D. & Cheilletz, A. Emerald mineralisation in
    Colombia: fluid chemistry and the role of brine mixing. Miner. Deposita 35, 699–713
    (2000b).

Bottomley, D. J., Katz, A., Chan, L. H., Starinsky, A., Douglas, M., Clark, I .D. & Raven, K.G.
    The origin and evolution of Canadian Shield brines: evaporation or freezing of seawater?
    New lithium isotope and geochemical evidence from the Slave craton. Chem. Geol. 155,
    295–320 (1999).

Burisch, M., Walter, B. F., Wälle, M. & Markl, G. Tracing fluid migration pathways in the root
    zone below unconformity-related hydrothermal veins: Insights from trace element
    systematics of individual fluid inclusions. Chem. Geol. 429, 44–50 (2016a).

Burisch, M., Marks, M. A., Nowak, M. & Markl, G. The effect of temperature and cataclastic
    deformation on the composition of upper crustal fluids – An experimental approach.
    Chemical Geology 433, 24–35 (2016b).

Campbell, A. R., Banks, D. A., Phillips, R. S. & Yardley, B. W. D. Geochemistry of Th-U-REE
    mineralising magmatic fluids, Capitan Mountains, New Mexico. Econ. Geol. 90, 1271–
    1287 (1995).

Chan, L. H., Edmond, J. M. & Thompson, G. A lithium isotope study of hot springs and
    metabasalts from mid-ocean ridge hydrothermal systems. J. Geophys. Res. 98, 9653–9659
    (1993).

Chan, L. H. & Kastner, M. Lithium isotopic compositions of pore fluids and sediments in the
    Costa Rica subduction zone: implications for fluid processes and sediment contribution to
    the arc volcanoes. Earth Planet. Sci. Lett. 183, 275–290 (2000).

Derome, D., Cathelineau, M., Fabre, C., Boiron, M. C., Banks, D., Lhomme, T. & Cuney, M.
    Paleo-fluid composition determined from individual fluid inclusions by Raman and LIBS:

Application to mid-proterozoic evaporitic Na-Ca brines (Alligator Rivers Uranium Field, northern territories Australia). Chem. Geol. 237, 240–254 (2007).

Deveaud, S., Millot, R. & Villaros, A. The genesis of LCT-type granitic pegmatites, as illustrated by lithium isotopes in micas. Chem. Geol. 411, 97–111 (2015).

Drever, J. I. The Geochemistry of Natural Waters. Prentice-Hall, Englewood Cliffs, N.J., 388 pp. (1982).

Dolejš, D. Quantitative characterization of hydrothermal systems and reconstruction of fluid fluxes: the significance of advection, disequilibrium, and dispersion in Mineral Resources in a Sustainable World. Proceedings of the 13th Biennial SGA Meeting, 24-27 August 2015, Nancy, France, Vol. 2 (eds André-Mayer, A. S., Cathelineau, M., Muchez, P., Pirard, E. & Sindern, S.) 445–448 (SGA, 2015).

Flesch, G. D., Anderson, A. R. J. & Svec, H. J. A secondary isotopic standard for $^6Li/^7Li$ determinations. Int. J. Mass Spectrom. 12, 265–272 (1973).

Fontes, J. C. & Matray, J. M. Geochemistry and origin of formation brines from the Paris Basin, France 1. Brines associated with Triassic salts. Chem. Geol. 109, 149–175 (1993).

Foustoukos, D. I., James, R. H., Berndt, M. E. & Seyfried, J. W. E. Lithium isotopic systematics of hydrothermal vent fluids at the Main Endeavour Field, Northern Juan de Fuca Ridge. Chem. Geol. 212, 17–26 (2004).

Gao, Y., Vils, F., Cooper, K. M., Banerjee, N., Harris, M., Hoefs, J., Teagle, D. A. H., Casey, J. F., Elliott, T., Laverne, C., Alt, J. C. & Muehlenbachs, K. Downhole variation of lithium and oxygen isotopic compositions of oceanic crust at East Pacific Rise, ODP Site 1256. Geochem. Geophy. Geosy. 13, Q10001 (2012).

Gleeson, S. A., Wilkinson, J. J., Boyce A. J., Fallick, A. E. & Stuart, F. M. On the occurrence and wider implications of anomalously low δD fluids in quartz veins, South Cornwall, England. Chem. Geol. 160, 161–173 (1999).

Godfrey, L. V., Chan, L. H., Alonso, R. N., Lowenstein, T. K., McDonough, W. F., Houston, J., Bobst, A. & Jordan, T. E. The role of climate in the accumulation of lithium-rich brine in the Central Andes. Appl. Geochem. 38, 92–102 (2013).

Götze, J., Plötze, M., Graupner, T., Hallbauer, D. K. & Bray, C. Trace element incorporation into quartz: A combined study by ICP-MS, electron spin resonance, cathodoluminescence, capillary ion analysis, and gas chromatography. Geochim. Cosmochim. Acta 68, 3741–3759 (2004).

Guillong, M., Meier, D. L., Allan, M., Heinrich, C.A. & Yardley, B. W. D. SILLS: A Matlab-based program for the reduction of laser ablation ICP-MS data of homogeneous materials and inclusions in Mineralogical Association of Canada Short Course Series 40: Laser Ablation ICP–MS in the Earth Sciences: Current Practices and Outstanding Issues (ed Sylvester, P.) 328–333 (Mineralogical Association of Canada, 2008).

Halama, R., John, T., Herms, P., Hauff, F. & Schenk, V. A stable (Li, O) and radiogenic (Sr, Nd) isotope perspective on metasomatic processes in a subducting slab. Chem. Geol. 281, 151–166 (2011).

Huh, Y., Chan, L. H., Zhang, L. & Edmond, J. M. Lithium and its isotopes in major world rivers: implications for weathering and the oceanic budget. Geochim. Cosmochim. Acta 62, 2039–2051 (1998).

Jahn, S. & Wunder, B. Lithium speciation in aqueous fluids at high P and T studied by ab initio molecular dynamics and consequences for Li-isotope fractionation between minerals and fluids. Geochim. Cosmochim. Acta 73, 5428–5434 (2009).

Kendrick, M. A. & Burnard, P. Noble gases and halogens in fluid inclusions: A journey through the Earth's crust in The Noble Gases as Geochemical Tracers (ed Burnard, P.) 319–369 (Springer-Verlag, 2013).

Lambrecht, G. & Diamond, L. W. Morphological ripening of fluid inclusions and coupled zone-refining in quartz crystals revealed by cathodoluminescence imaging: Implications for CL-petrography, fluid inclusion analysis and trace-element geothermometry. Geochim. Cosmochim. Acta 141, 381–406 (2014).

Liebscher, A., Meixner, A., Romer, R. L. & Heinrich, W. Experimental calibration of the vapour–liquid phase relations and lithium isotope fractionation in the system H_2O–LiCl at 400°C/20–28 MPa. Geofluids 7, 369–375 (2007).

Lynton, S. J., Walker, R. J. & Candela, P. A. Lithium isotopes in the system Qz-Ms-fluid: An experimental study. Geochim. Cosmochim. Acta. 69, 3337–3347 (2005).

Masukawa, K., Nishio, Y. & Hayashi, K. I. Lithium-strontium isotope and heavy metal content of fluid inclusions and origin of ore-forming fluid responsible for tungsten mineralization at Takatori mine, Japan. Geochem. J. 47, 309–319 (2013).

McCaig, A. M., Tritlla, J. & Banks, D. A. Fluid mixing and recycling during Pyrenean thrusting: Evidence from fluid inclusion halogen ratios. Geochim. Cosmochim. Acta 64, 3395–3412 (2000).

Meynadier, L., Gorge, C., Birck, J. L. & Allègre, C. J. Automated separation of Sr from natural water samples or carbonate rocks by high performance ion chromatography. Chem. Geol. 227, 26–36 (2006).

Millot, R., Guerrot, C. & Vigier, N. Accurate and high precision measurement of lithium isotopes in two reference materials by MC-ICP-MS. Geostand. Geoanal. Res. 28, 53–159 (2004).

Millot, R. & Négrel, P. Multi-isotopic tracing (δ^7Li, δ^{11}B, ^{87}Sr/^{86}Sr) and chemical geothermometry: evidence from hydro-geothermal systems in France. Chem. Geol. 244, 664–678 (2007a).

Millot, R., Négrel, P. & Petelet-Giraud, E. Multi-isotopic (Li, B, Sr, Nd) approach for geothermal reservoir characterization in the Limagne Basin (Massif Central, France). Appl. Geochem. 22, 2307–2325 (2007b).

Millot, R., Petelet-Giraud, E., Guerrot, C. & Négrel, P. Multi-isotopic composition (δ^7Li–δ^{11}B– δD–δ^{18}O) of rainwaters in France: origin and spatio-temporal characterization. Appl. Geochem. 25, 1510–1524 (2010a).

Millot, R., Scaillet, B. & Sanjuan, B. Lithium isotopes in island arc geothermal systems: Guadeloupe, Martinique (French West Indies) and experimental approach. Geochim. Cosmochim. Acta 74, 1852–1871 (2010b).

Millot, R., Hegan, A. & Négrel, P. Geothermal waters from the Taupo Volcanic Zone, New Zealand: Li, B and Sr isotopes characterization. Appl. Geochem. 27, 677–688 (2012).

Monecke, T., Kempe, U. & Götze, J. Genetic significance of the trace element content in metamorphic and hydrothermal quartz: a reconnaissance study. Earth Plan. Sc. Lett. 202, 709–724 (2002).

Munz, I. A., Yardley, B. W. D., Banks, D. A. & Wayne, D. Deep penetration of sedimentary fluids in basement rocks from southern Norway: evidence from hydrocarbon and brine inclusions in quartz rocks. Geochim. Cosmochim. Acta 59, 239–54 (1995).

Penniston-Dorland, S. C., Bebout, G. E., Pogge von Strandmann, P. A. E., Elliott, T. & Sorensen, S. S. Lithium and its isotopes as tracers of subduction zone fluids and metasomatic processes: Evidence from the Catalina Schist, California, USA. Geochim. Cosmochim. Acta 77, 530–545 (2012).

Pettke, T. & Diamond, L. W. Rb-Sr isotopic analysis of fluid inclusions in quartz: Evaluation of bulk extraction procedures and geochronometer systematics using synthetic fluid inclusions. Geochim. Cosmochim. Acta 59, 4009–4027 (1995).

Pettke, T., Diamond, L. W. & Jan, D. Kramers. Mesothermal gold lodes in the north-western Alps. Eur. J. Mineral. 12, 213–230 (2000).

Pettke, T., Oberli, F. & Heinrich, C. A. The magma and metal source of giant porphyry-type ore deposits, based on lead isotope microanalysis of individual fluid inclusions. Earth Planet. Sci. Lett. 296, 267–277 (2010).

Polya, D. A., Foxford, K. A., Stuart, F., Boyce, A. & Fallick, A. E. Evolution and paragenetic context of low δD hydrothermal fluids from the Panasqueira W-Sn deposit, Portugal: new evidence from microthermometric, stable isotope, noble gas and halogen analyses of primary fluid inclusions. Geochim. Cosmochim. Acta 64, 3357–3371 (2000).

Richard, A., Banks, D. A., Mercadier, J., Boiron, M. C., Cuney, M. & Cathelineau, M. An evaporated seawater origin for the ore-forming brines in unconformity-related uranium deposits (Athabasca Basin, Canada): Cl/Br and δ^{37}Cl study of fluid inclusions. Geochim. Cosmochim. Acta 75, 2792–2810 (2011).

Richard, A., Kendrick, M. A. & Cathelineau, M. Noble gases (Ar, Kr, Xe) and halogens (Cl, Br, I) in fluid inclusions from the Athabasca Basin (Canada): Implications for unconformity-related U deposits. Precambrian Res. 247, 110–125 (2014).

Romer, R. L., Heinrich, W., Schröder-Smeibidl, B., Meixner, A., Fischer, C. O. & Schulz C. Elemental dispersion and stable isotope fractionation during reactive fluid-flow and fluid immiscibility in the Bufa del Diente aureole, NE-Mexico: evidence from radiographies and Li, B, Sr, Nd, and Pb isotope systematic. Contrib. Mineral. Petrol. 149, 400–429 (2005).

Schmitt, A. D., Vigier, N., Lemarchand, D., Millot, R., Stille, P. & Chabaux, F. Processes controlling the stable isotope compositions of Li, B, Mg and Ca in plants, soils and waters: a review. C. R. Geosci. 344, 704–722 (2012).

Scholz, F., Hensen, C., De Lange, G. J., Haeckel, M., Liebetrau, M., Meixner, A., Reitz, A. & Romer, R. L. Lithium isotope geochemistry of marine pore waters – Insights from cold seep fluids. Geochim. Cosmochim. Acta 74, 3459–3475 (2010).

Sturchio, N. C. & Chan, L. H. Lithium isotope geochemistry of the Yellowstone hydrothermal system. Soc. Econ. Geol. Spec. Pub. 10, 171–180 (2003).

Teng, F. Z., McDonough, W. F., Rudnick, R. L., Dalpé, C., Tomascak, P. B., Chappell, B. W. & Gao, S. Lithium isotopic composition and concentration of the upper continental crust. Geochim. Cosmochim. Acta 68, 4167–4178 (2004).

Teng, F. Z., McDonough, W. F., Rudnick, R. L., Walker, R. J. & Sirbescu, M. L. C. Lithium isotopic systematics of granites and pegmatites from the Black Hills, South Dakota. Am. Mineral. 91, 1488–1498 (2006a).

Teng, F. Z., McDonough, W. F., Rudnick, R. L. & Walker, R. J. Diffusion-driven extreme lithium isotopic fractionation in country rocks of the Tin Mountain pegmatite. Earth Planet. Sci. Lett. 243, 701–710 (2006b).

Tester, J. W., Worley, W. G., Robinson, B. A., Grigsby, C. O. & Feerer, J. L. Correlating quartz dissolution kinetics in pure water from 25 to 625°C. Geochim. Cosmochim. Acta 58, 2407– 2420 (1994).

Tomascak, P. B., Magna, T., & Dohmen, R. Advances in Lithium Isotope Geochemistry (ed Hoefs, J.) 195 pp (Springer International Publishing, 2016).

Turner, G. & Bannon, M. P. Argon isotope geochemistry of inclusion fluids from granite-associated mineral veins in southwest and northeast England. Geochim. Cosmochim. Acta 56, 227–243 (1992).

Wunder, B., Meixner, A., Romer, R. L., Feenstra, A., Schettler, G. & Heinrich, W. Lithium isotope fractionation between Li-bearing staurolite, Li-mica and aqueous fluids: An experimental study. Chem. Geol. 238, 277–290 (2007).

Yang, D., Hou, Z., Zhao, Y., Hou, K., Yang, Z., Tian, S. & Fu, Q. Lithium isotope traces magmatic fluid in a seafloor hydrothermal system. Sci. Rep. 5, 13812 (2015).

Yardley, B. W. D., Banks, D. A., Bottrell, S. H. & Diamond, L. W. Post-metamorphic gold-quartz veins from N.W. Italy: the composition and origin of the ore fluid. Mineral Mag. 57, 407–422 (1993).

Yardley, B. W. & Bodnar, R. J. Fluids in the continental crust. Geochemical Perspectives 3, 1–123 (2014).

Zajacz, Z., Hanley, J. J., Heinrich, C. A., Halter, W. E. & Guillong, M. Diffusive reequilibration of quartz-hosted silicate melt and fluid inclusions: Are all metal concentrations unmodified? Geochim. Cosmochim. Acta 73, 3013–3027 (2009).

Table captions

Table 1: Provenance, reference sample, mineralogy, fluid inclusions trapping temperatures and average salinities of the selected samples. All data have been published as indicated. [a] Samples from Southwest England are paragenetically equivalent to samples from Sn-W mineralisation and Cu-Pb-Zn mineralisation stages (Alderton and Harmon, 1991). [b]

Samples from the Panasqueira W-Sn deposit (Portugal) are paragenetically equivalent or the same samples as from the "main sulfide stage / pyrrotite alteration stage" (MSS/PAS) (Polya et al., 2000).

Table 2: Analytical results. RSD: relative standard deviation. [a] Out of calibration range. [b] Not measured (irrelevant in carbonate minerals). [c] Br/Cl and I/Cl values have been published as detailed in Table 1 except for the followings: I/Cl values of samples MAC5Qz, RBL5Qz and RBL5Carb have been attributed to published values obtained on the paragenetically equivalent samples, respectively MAC54Qz, RBL7Qz and RBL7Carb (Richard et al., 2014); Br/Cl and I/Cl values of the four samples from Southwest England (HW1068F, SW18, WCO, and FI37) and the two samples from Panasqueira Sn-W deposit have been obtained from ion chromatography in this study. Missing I/Cl values indicate that iodine was below limit of detection (except for sample CA 00-1 for which no analysis was done). [d] Absolute Li concentrations in fluid inclusions are reconstructed using a charge-balance approach (see Section 2.5.).

Figure captions

Figure 1: δ^7Li value vs Li concentration for fluid inclusions (this study) and various fluid samples from other contributions. Error bars are plotted at $\pm$ 10% for all Li concentrations and $\pm$ 1‰ (> 1σ) for all for δ^7Li values. Reference data: modern seawater (Millot et al., 2004); evaporated seawater, taken as beyond halite saturation and considering negligible isotopic fractionation during evaporation and salt precipitation (Fontes and Matray, 1993); meteoric waters (Huh et al., 1998; Millot et al., 2010a); UCC: upper continental crust

(Teng et al., 2004); geothermal waters (Sturchio and Chan, 2003; Millot et al., 2007a,b, 2010b, 2012); SHDH fluids: sediment-hosted diagenetic and hydrothermal fluids (compilation, Scholz et al., 2010); MORV fluids: mid-ocean ridge vent fluids (compilation, Scholz et al., 2010). Trends between meteoric water, seawater, evaporated seawater and upper continental crust (UCC) represent binary mixing lines between the different reservoirs (Scholz et al., 2010). Fluid composition during progressive Li incorporation into authigenic clay minerals at 150°C and 350°C are calculated using a Rayleigh fractionation model and represented for different fractions of the initial Li remaining in the fluid (between 1 and 0.1; Scholz et al., 2010).

Figure 2: $Li_{fluid\ inclusions}$ (a) and $\delta^7Li_{fluid\ inclusions}$ (b) vs $Li_{host\ mineral}$; $\delta^7Li_{fluid\ inclusions}$ vs trapping temperature (c), salinity (d) and Br/Cl (e), I/Cl (f), Na/Ca (g), Na/K (h), Na/Mg (i), Na/Li (j), Na/Sr (k) molar ratios for the studied fluid inclusions. The symbol size exceeds the analytical uncertainties except for I/Cl ratios which are semi-quantitative. * Regression line of temperature vs δ^7Li data from some hydro-geothermal systems in France (Millot and Négrel, 2007a). Empty stars stand for modern seawater composition (Drever, 1982; Millot et al., 2004). Black bars stand for the range of composition of the upper continental crust (Teng et al., 2004).
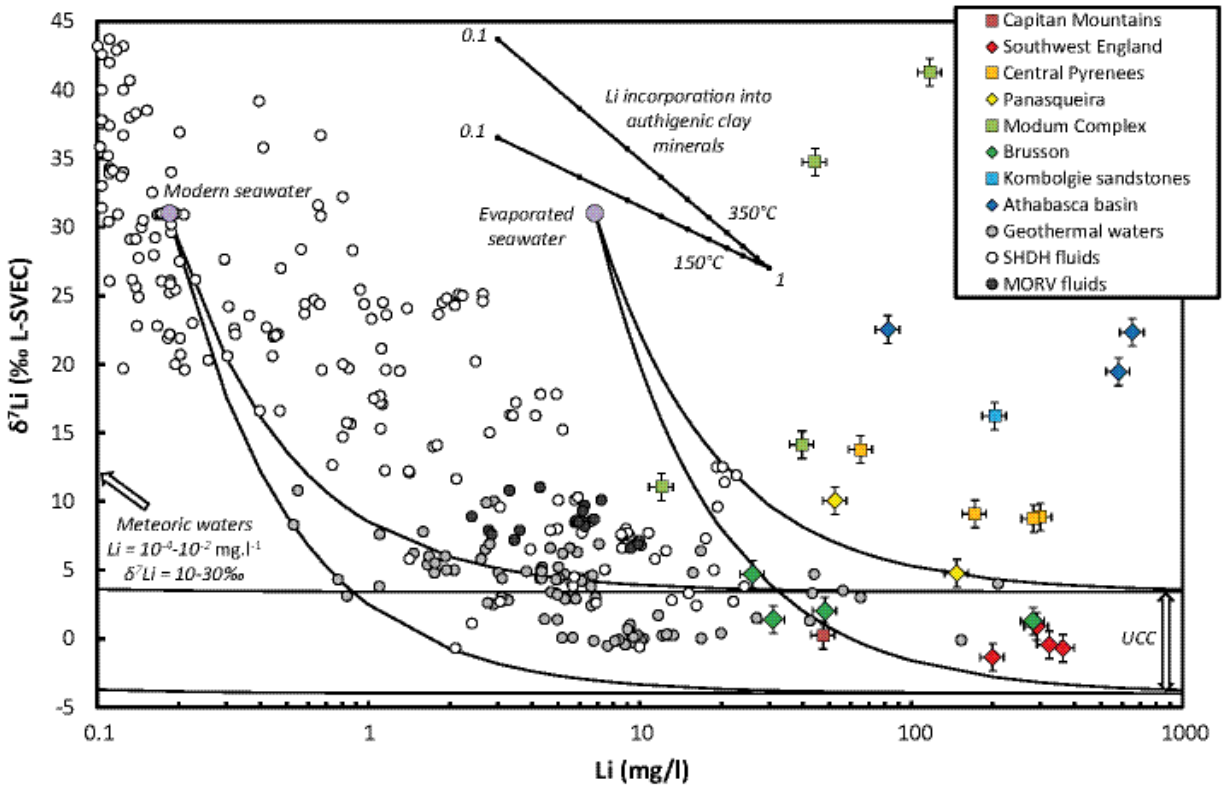
Figure 1
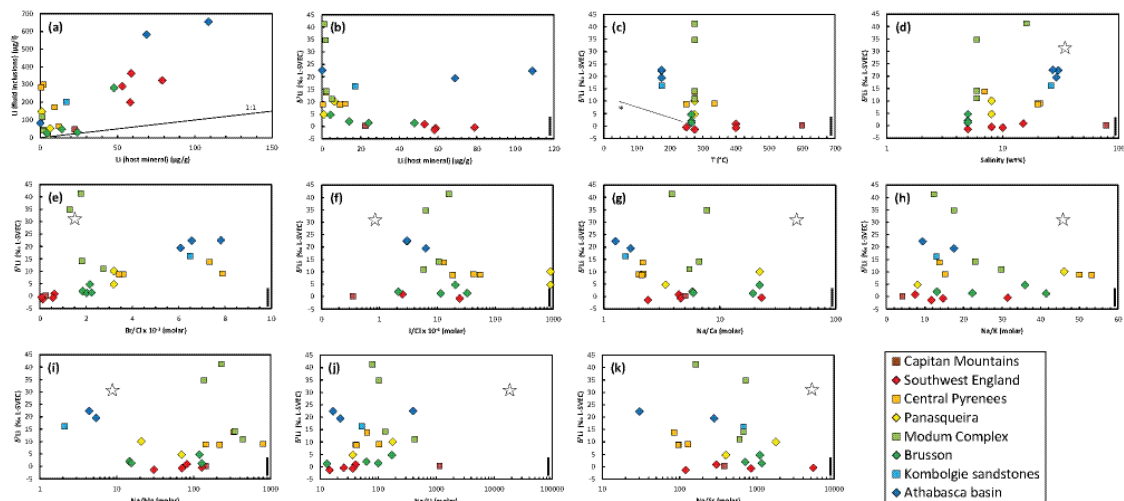
Figure 2

Table 1

Locality		Reference samples	Host mineral	Temperature of trapping (°C)	Average salinity (wt.% equiv. NaCl)	Source
Capitan Mountains (U.S.A.)	-	MTE	Quartz	600	78	Campbell et al. (1995)
Southwest England [a]	Hemerdon (Sn-W mineralisation)	HW1068F	Quartz	400	15	Alderton and Harmon (1991)
	Gunnislake (Sn-W mineralisation)	SW18	Quartz	400	10	Turner and Bannon (1992)
	Perran Wheal George (Cu-Pb-Zn mineralisation)	FI37	Quartz	275	5	Alderton and Harmon (1991)
	Wheal Cook (Cu-Pb-Zn mineralisation)	WCO	Quartz	250	8	Alderton and Harmon (1991)
Central Pyrenees (France)	La Glère (Néouvielle)	N90-6	Quartz	310-360	21	McCaig et al. (2000)
	Plan de Larri	PL90-9d2	Quartz	250-300	7	McCaig et al. (2000)
	Pic de Port Vieux	52763-m	Quartz	200-300	20	McCaig et al. (2000)
	Pic de Port Vieux	IH31C	Quartz	200-300	20	McCaig et al. (2000)
Panasqueira W-Sn deposit (Portugal) [b]	-	MSS/PAS1	Quartz	250-300	8	Polya et al. (2000)
	-	MSS/PAS2	Quartz	250-300	8	Polya et al. (2000)
Modum Complex (Norway)	-	IA-463	Quartz	250-300	6	Munz et al. (1995)
	-	DØV-1	Quartz	250-300	6	Munz et al. (1995)
	-	IA-527	Quartz	250-300	6	Munz et al. (1995)
	-	IA-511G	Quartz	250-300	16	Munz et al. (1995)
Brusson Au district (Italy)	-	LD659	Quartz	230-300	5	Yardley et al. (1993)
	-	LD671	Quartz	230-300	5	Yardley et al. (1993)

32

	-	LD88 8	Qua rtz	230-300	5	Yardley et al. (1993)
	-	LD91 0	Qua rtz	230-300	5	Yardley et al. (1993)
Kombolgie sandstones (Australia)	Caramal U deposit	CA 00-1	Qua rtz	150-200	26	Derome et al. (2007)
Athabasca basin (Canada)	McArthur River U deposit	MAC 5Qz	Qua rtz	150-200	29	Richard et al. (2011)
	Rabbit Lake U deposit	RBL 5Qz	Qua rtz	150-200	30	Richard et al. (2011)
	Rabbit Lake U deposit	RBL 5Car b	Dol omi te	150-200	27	Richard et al. (2011)

Table 2

Locality	Reference samples	Host minerals	Li (μg/g)	1σ	RSD (%)	LD (μg/l)	Na (mg/l)	K (mg/l)	Mg (mg/l)	Ca (mg/l)	Sr (μg/l)	Na/Li (molar)	Na/K (molar)	Na/Mg (molar)	Na/Ca (molar)	Na/Sr (molar)	Br/Cl [c] ($\times 10^{-3}$ molar)	I/Cl [c] ($\times 10^{-6}$ molar)	δ^7Li ‰ L-SVEC	1σ	Fluid inclusions [d] Li (mg/l)
Capitan Mountains (U.S.A.)	MTE	–	22.2	1.7	7.4	8.8	32.90	13.32	0.24	11.38	332.4	3138	14	143	5	379	0.3	0.3	0.2	0.2	47
Southwest England	HW1068F	Hemerdon (Sn-W mineralisation)	53.1	21.5	40.4	69.3	9.34	2.12	0.12	3.67	119.2	41	87	301	4	0	0.06	3	0.9	0.3	290
	SW18	Gunnislake (Sn-W mineralisation)	58.8	8.6	4.7	8.3	1.38	2.39	3.05	0.28	5.4	1836	115	71	45	0	0.6	24	-0.7	0.2	363
	FI37	Perran Wheal George (Cu-Pb-Zn mineralisation)	58.3	9.2	5.8	9.3	1.79	7.55	3.13	0.74	101.3	215	212	30	22	0	0.1	-	-1.4	0.2	200
	WCO	Wheal Cook (Cu-Pb-Zn mineralisation)	78.9	8.0	2.8	5.7	2.24	0.66	0.10	0.93	18.7	126	31	28	23	0.1	-	-0.5	0.2	323

ation)

Region	Site	Sample	Data (stacked digits)	Total
Central Pyrenees (France)	La Glère (Néouvielle)	N90-6	2 / 5 6 3 2 0 8 8 / 9 5 8 8 . . . . 0 1 8 1 0 / . . . . 0 5 0 3 . 0 1 0 2 7. 9. . / 3 4 6 0 1 7 3 3 2 3 5 0 2 9 9 41 1 4	172
	Plan de Larri	PL90-9d2	1 2 / 1 1 1 5 3 0 0 3 / 1 2 2 7 9 . . . . 5 3 1 0 / . . . . 1 1 0 1 . 6 1 2 8 7. 3. . / 0 1 4 3 7 0 8 9 0 4 4 8 2 5 3 13 8 2	65
	Pic de Port Vieux	52763-m	1 1 4 / 4 9 2 0 0 0 8 / 2 0 3 1 . . . . 7 1 0 / . . . . 3 4 0 7 . 4 5 4 9 3. 8. . / 2 9 4 6 8 2 9 0 1 1 0 4 2 7 6 55 9 4	299
	Pic de Port Vieux	IH31C	1 1 6 / 1 1 6 0 0 3 6 / 0 0 2 8 . . . . 0 2 0 / . . . . 6 5 0 5 . 4 5 1 9 3. 8. . / 5 1 1 8 2 3 8 9 6 3 3 7 2 6 4 18 7 3	283
Panasqueira W-Sn deposit (Portugal)	-	MSS/PAS1	4 1 1 0 0 0 1 / 1 0 4 1 . . . . 2 3 0 / . . . . 3 2 0 6 . 3 6 9 3. 90 4. 0 / 0 4 1 1 3 8 2 8 8 6 8 9 3 8 2 0 8 5	147
	-	MSS/PAS2	1 5 0 0 0 1 / 6 0 9 0 . . . . 3 1 1 1 0 / . . . . 9 2 3 4 . 7 4 2 2 6 3. 90 0. . / 4 6 3 3 8 2 0 7 0 7 6 1 2 0 2 0 1 2	52
Modum Complex (Norway)	-	IA-463	1 / 4 3 0 1 0 2 5 / 1 0 5 1 . . . . 5 1 1 7 3 0 / . . . . 4 0 0 3 . 0 1 3 2 1. 4. . / 8 8 3 1 2 1 8 3 4 2 7 6 8 0 3 6 7 2	44
	-	DØV-1	4 / 2 2 1 2 0 3 6 / 5 1 5 9 . . . . 6 4 4 5 1 0 / . . . . 6 3 1 2 . 2 3 3 9 2. 1. . / 1 3 7 8 0 7 0 3 5 5 0 4 5 7 7 6 1 3	12
	-	IA-527	2 0 1 6 2 1 0 6 1 1 3 1 0 / . . 7 0 5 . . . 4 3 2 3 7 1. 4. . / 1 4 . . . 9 0 8 7 1 3 8 7 3 8 11 1 7	40

Region	Deposit	Sample	Data (as read)	Last col
Brusson Au district (Italy)	-	IA-511-G	471.3 320.9 961.9 105.2 80.59 12.91 … 0.28 … 1.61 … 16 … 41.3 … 08	117
	-	LD659	414.26 149.51 251.48 613.82 0.77 1.72 4.07 … 2.02 … 20 … 47.3	26
	-	LD671	428.2 106.53 865.34 823.22 7.16 6.6 2.27 … 1.08 … 9 2 … 2.03	48
	-	LD888	47.8 178.34 834.42 442.9 20.25 01.11 13.17 29.1 … 2.0 … 11 … 1.35	281
	-	LD910	42.17 01.89 287.79 67.90 0.02 21.4 0.25 68.2 … 32 … 41.5	31
Kombolgie sandstones (Australia)	Caramal U deposit	CA00-1	17.0 12.05 44.54 89.49 05.3 20.0 47.6 77.3 … 65.12 … 67.23 … 1 … 6.24	203
Athabasca basin (Canada)	McArthur River U deposit	MAC5Qz	68.8 2.7 23.9 32.7 19.3 0.39 08.5 09.1 … 26 … 12.28 … 85.20 … 1 16 … 19.5	582
	Rabbit Lake U deposit	RBL5Qz	10.8 06.9 93.0 60 … 95.6 09.5 … 01.6 76.4 … 45.7 … 79.4 … 10 … 3 … 23.4	653
	Rabbit Lake U deposit	RBL5Carb	00.7 00.1 41.3 75 … 98.4 (a) (b) (b) (b) … 39.9 … 7.8 … 3 … 2.52	82

Graphical abstract

Highlights

. Li isotope systematics of fluid inclusions is explored

. Fluid inclusions from a variety of deep (~ 150 to 600°C) environments are selected

. Crush-leach, high-performance ion chromatography and MC-ICPMS are combined

. First overview of Li isotopic compositions in fluid inclusions is provided

. Li isotopes in fluid inclusions are potentially powerful tracers of deep fluids